

# Effect of Plasma Spraying Process on Microstructure and Microhardness of Titanium Alloy Substrate

H. Zhou, F. Li, B. He, J. Wang, and B. Sun

(Submitted March 23, 2007; in revised form June 15, 2007)

High-temperature titanium alloys are considered as good candidate materials for many aerospace applications. In order to increase the usable temperatures and oxidation resistance of titanium alloys, plasma spraying thermal barrier coatings (TBCs) on the titanium alloys is considered as an effective method. The effect of plasma spraying process on microstructure and microhardness of the titanium alloy (Ti-6.6Al-3.61Mo-1.69Zr-0.28Si in wt.%) was investigated by scanning electron microscope, energy dispersion analytical X-ray spectroscopy (EDAX) and microhardness test. The results show that the microstructure of the titanium alloy inside the substrate keeps unchanged after plasma spraying, and no interaction and atomic diffusion happen evidently at the bond coat/substrate interface. However there exists a thin layer of plastic deformation zone in the substrate beneath the bond coat/substrate interface after plasma spraying. The residual stresses are induced inside the titanium alloy due to the thermal expansion mismatch and the temperature gradient inside the substrate during plasma spraying, and lead to generating microcracks in the surface beneath the bond coat/substrate interface and the increase of microhardness in the substrate.

**Keywords** microhardness, microstructure, plasma spraying, titanium alloy

## 1. Introduction

As lightweight structural materials, titanium and its alloys have been widely used in aircraft, automobile, and space industries. The applications of titanium alloy are mainly focused on its superior strength, ductility, and creep resistance at room and high temperatures as well as unique corrosion resistance and non-magnetic properties. For some of those applications a high-temperature capability of above 800 °C is required in order to meet advanced engine design goals. The upper temperature limit of the best conventional high-temperature titanium alloy, usually from the class of near  $\alpha$  alloy, is approximately 600 °C since the conventional titanium alloys form a non-protective oxide scale consisting of a heterogeneous mixture of alumina and titania during high-temperature exposure to oxidizing atmospheres. The affinity of titanium for oxygen is one of the main factors that deteriorate the application of titanium alloys as structural materials at elevated temperatures. Oxidation

results in the loss of material by oxide scale growth and embrittlement of the alloy by dissolved oxygen. Deposition of protective and thermally insulating coatings that serve as oxygen barriers is in principle considered as an effective means to reduce the substrate's temperature and suppress both oxidation- and oxygen-induced embrittlement (Ref 1-3). Research work undertaken in the past decade also showed that it was a more effective method by the protective coatings to provide improved oxidation resistance to titanium alloys than by alloying (Ref 4).

Thermal barrier coatings (TBCs) have been successfully used onto the nickel-based superalloy substrates in recent decades. The primary function of TBCs is to provide thermal protection to metallic components from hot gas stream in gas-turbine engines due to their low-thermal conductivity and thermal diffusivity combined with proper chemical stability at high temperatures. Conventional TBCs usually consist of a layer of low-thermal conductivity ceramic coating, which is commonly a yttria partially stabilized zirconia (YPSZ) and a layer of MCrAlY (M=Ni and/or Co) bond coat which possesses the properties of not only excellent oxidation and hot corrosion resistances but also sufficient toughness (Ref 5-7).

In the present work, 8 wt.% YPSZ TBCs were deposited by air plasma spraying on titanium alloy substrates. The microstructures and microhardnesses of the titanium alloy before and after plasma spraying were studied. The aim of the research is to study the effect of plasma spraying on the changes of the microstructure and mechanical properties of the titanium alloy.

H. Zhou, F. Li, B. He, J. Wang, and B. Sun, State Key Laboratory of Metal Matrix Composites, Shanghai Jiao Tong University, Shanghai China. Contact e-mail: zhou7210@yahoo.com.cn

## 2. Experimental

### 2.1 Sample Preparation

Annealed state titanium alloy disks (Ti-6.6Al-3.61 Mo-1.69Zr-0.28 Si in wt.%) with 80 mm in diameter and 3 mm in thickness were used as the substrates in the work. The substrates were grit blasted with alumina, ultrasonically cleaned in anhydrous ethylene alcohol and dried in cold air prior to coating deposition. Commercially available 8 wt.%  $Y_2O_3$ -ZrO<sub>2</sub> ceramic feedstock powder (HHZrO-8, Chinese Academy of Agricultural Mechanization Science, Beijing, China) with particle sizes ranging from 38.5 to 63  $\mu\text{m}$  and NiCrAlY metal powder (HHNiCrAlY-9, Chinese Academy of Agricultural Mechanization Science, Beijing, China) with particle sizes in the range of 10–100  $\mu\text{m}$  were used. A NiCrAlY bond coat with about 100  $\mu\text{m}$  in thickness was atmospherically plasma sprayed onto the titanium alloy substrate before the 300  $\mu\text{m}$  YPSZ top coating was deposited by using the same air plasma spray system (DH80, Chinese Academy of Agricultural Mechanization Science, Beijing, China). No air cooling on the backside of the substrates was applied during the plasma spraying process. The temperatures of the substrate backside were measured with an infrared thermometer (F68, FLUKE, USA) during the spraying process. The spraying parameters are given in Table 1.

### 2.2 Microstructure Observation and Microhardness Test

The microstructures of the substrate and the interfacial morphology were investigated using a field emission scanning electron microscope (FESEM, Model Sirion 200), equipped with an energy dispersion analytical X-ray spectroscopy (EDAX, Oxford INCA, High Wycombe, UK), which was used for the analyses of element area distribution, and a Leco-I32A optical microscope with an image analysis system (LECO Corporation, St. Joseph).

The microhardness test was performed using a Vickers indenter (HXD-1000A, Shanghai, China) with a load of 100 g for a dwell time of 15 s for the substrates. The cross sections were polished before the indentations and the distance between the two indentations was at least three times the diagonal to prevent stress-field effects from nearby indentations. The microhardness value for the

**Table 1** Plasma spraying parameters for the TBCs

	NiCrAlY	YPSZ
Current, A	480	510
Voltage, V	65	75
Primary gas, Ar, l·min <sup>-1</sup>	37	...
Primary gas, N <sub>2</sub> , l·min <sup>-1</sup>	...	37
Secondary gas, H <sub>2</sub> , l·min <sup>-1</sup>	5	5
Powder feeding rate, g·min <sup>-1</sup>	50	15
Torch traverse speed, mm·s <sup>-1</sup>	10	6
Substrate rotation speed, rpm	126	126
Stand off distance, mm	100	60

substrate was taken from the average value of all measurement points. Ten measurement points that were distributed evenly along the thickness of the substrate were selected to observe the variation of microhardness.

## 3. Results and Discussion

### 3.1 Microstructure of the Substrate

The substrate, which is an  $\alpha + \beta$  type titanium alloy, can be used for long term at the temperature of 500 °C. Figure 1 shows the microstructures of the titanium alloy substrate before and after plasma spraying. It reveals that the substrate is composed of the  $\alpha$  phase with equiaxed grains and elongated grains, and the  $\beta$  phase which is distributed along the  $\alpha$  phase grain boundaries. The  $\alpha$  phase constitutes the dominative structure, representing more than 70% of the volume fraction of the substrate, as obtained by using the image analysis system. There is no obvious change of microstructure happened inside the

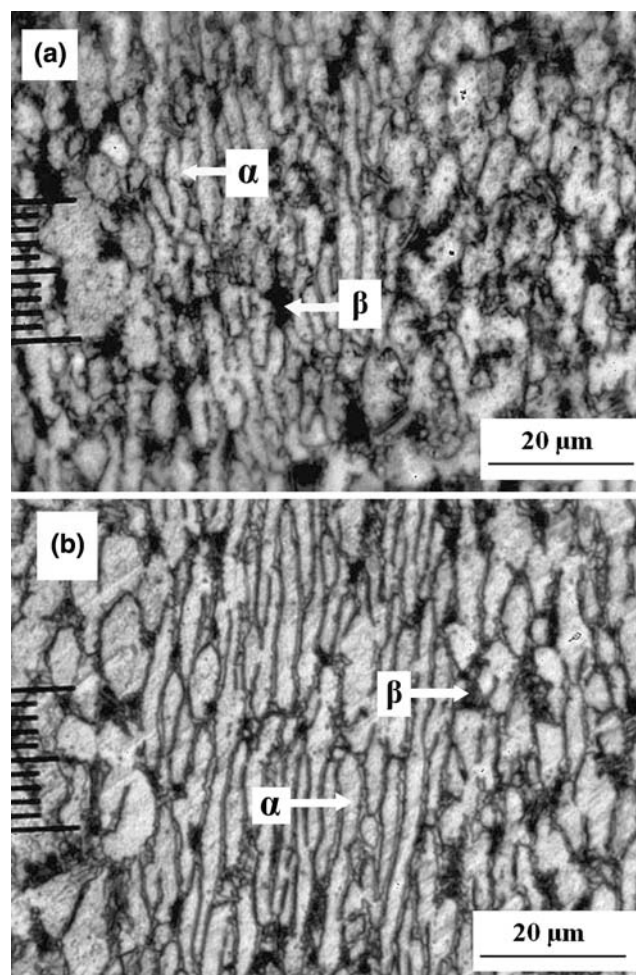


**Fig. 1** The microstructures of the internal substrate (a) before and (b) after thermal spraying

substrate after plasma spraying by comparison of the two microstructures of titanium alloy, as observed in Fig. 1. It results from the short period of heating process on the substrate and the moving of the spray gun and the substrate during plasma spraying, all which made the substrates stay at low temperatures, and keep the microstructure intact. The measured highest surface temperature on the disk backside during plasma spraying was 520 °C. The phase transformation temperature for this titanium alloy is  $1000 \pm 20$  °C (Ref 8). Therefore the microstructure of the internal substrate keeps unchanged after plasma spraying.

However, the surface of the substrate beneath the bond coat/substrate interface shows a different morphology in contrast to the substrate inside. A thin layer of plastic deformation zone exists evidently in the substrate surface, as shown in Fig. 2. The grains in the zone turn deformed to one direction with a river-like microstructure along the bond coat/substrate interface. It may be explained that during plasma spraying, the feedstock particles were sent and heated to above their melting point in the plasma jet. Next, the molten droplets with high temperatures were accelerated and impacted upon the rotating substrate surface which was moving normal to the plasma gun with a relative velocity in order to get a fully sprayed surface, and then passed the heat flux to the substrate surface, which could increase the transient temperature of the substrate surface to a high level. On the other hand, the substrate with 3 mm thickness, which was stiff and tough enough to prevent the disk from deformation during plasma spraying, limited the heat conduction through the substrate, and helped to increase its own temperature. Thus, the substrate surface was led to a near-molten state. With the cooperation of the impacting of high-speed molten droplets from one certain direction and the low-deformation resistance of the substrate surface at high temperatures, the plastic deformation zone beneath the bond coat/substrate interface was formed.

The thickness of the plastic deformation layer is non-uniform, as seen in Fig. 2. This phenomenon is related

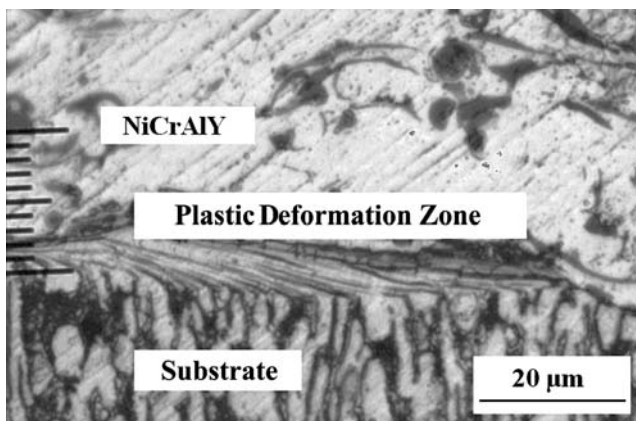


**Fig. 2** The thin layer of plastic deformation zone in the substrate surface after air plasma spraying

with the flattening ability of molten droplet and the inhomogeneous distribution of molten droplets during plasma spraying. The molten droplets got flattened after impinging on the substrate. However, the thickness of the flattened droplet was uneven with a thick core, and a thin brim. Therefore, the core with more heat would produce a thick plastic deformation zone, vice versa. The inhomogeneous distribution of molten droplets made the contact area and heat flux randomly distributed and resulted in the variation of thickness of the plastic deformation zone in the surface. In addition, the physical contact between the splat and the substrate is sometimes limited to several small contact areas, which also leads to the non-uniform thickness of the plastic deformation layer. Moreover, the spraying velocity and the scanning velocity also have an effect on the variation of thickness because they are connected with the energy input to the substrate.

Figure 3 shows the cross-sectional microstructure of a polished plasma-sprayed coating system and the element planar distribution around the bond coat/substrate interface after plasma spraying. It can be seen that the element distributions of Zr, Ni, and Ti have clear edges at the interfaces within the region and the atomic diffusion between different materials does not take place evidently. It can also be seen that the bond coat has a lamellar microstructure with pores, which is typical of microstructure of plasma spraying. During the spraying process, the molten droplets impinged upon the surface and flowed into thin splats, which adhered to the surface in an overlapping and interlocking fashion as they solidified, and then the lamellar structure was formed. The undulated interfaces related with the bond coat are clearly observed in Fig. 3. The undulations are favorable for adhesion of the interface by increasing the mechanical anchoring. However, they often induce imperfection, microcracks, and tensile stresses perpendicular to the interface, which cause the eventual failure of TBCs. Figure 4 shows the bond coat/substrate interface. Combined with the element distribution in Fig. 3, it can be obtained that the interface is clear, and there is not an interaction zone observed at the interface. The atomic diffusion between different materials did not take place evidently because of the short time at high temperature during plasma spraying. Therefore the interlocking mechanism is the main reason for the coating adhesion. Several microcracks are observed in the substrate beneath the bond coat/substrate interface from Fig. 4. The reason may be that the tensile stresses were generated on the substrate surface when the interface which was hotter than the internal substrate cooled down slower than the outside surface from high temperatures after thermal spraying. Moreover, the temperature gradient in the substrate, i.e., high temperature in the interface and low temperature at the backside of the substrate, which lead to generation of tensile stress in the bond coat/substrate interface as well during plasma spraying. When the maximum tensile stress was larger enough, the microcracks were initiated and propagated. Meanwhile, the existence of a thermal expansion coefficient mismatch of different materials also caused the crack formation.

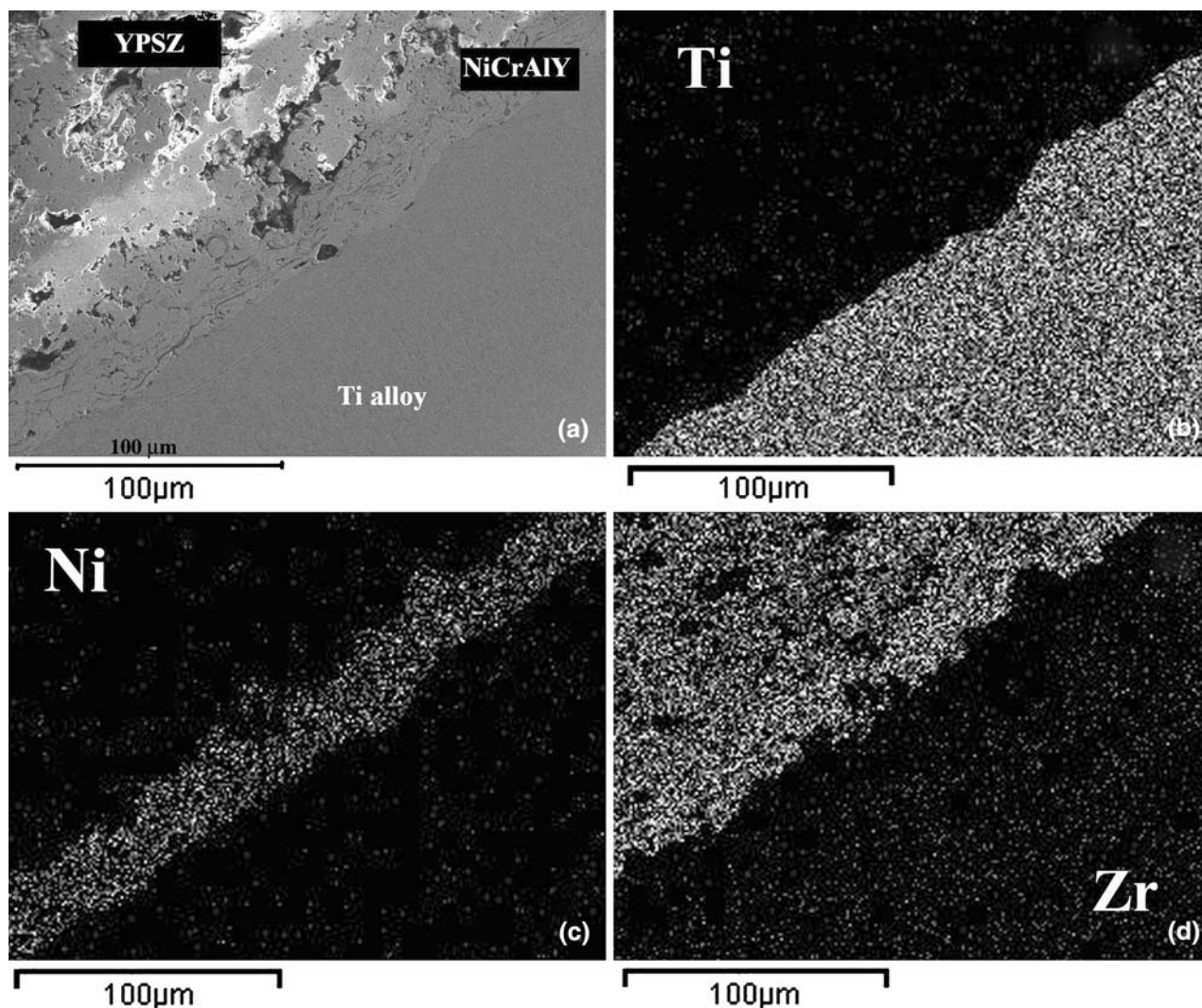


**Fig. 3** SEM morphology (a) and element planar distributions around the bond coat/substrate interface after plasma spraying (b), (c), and (d)

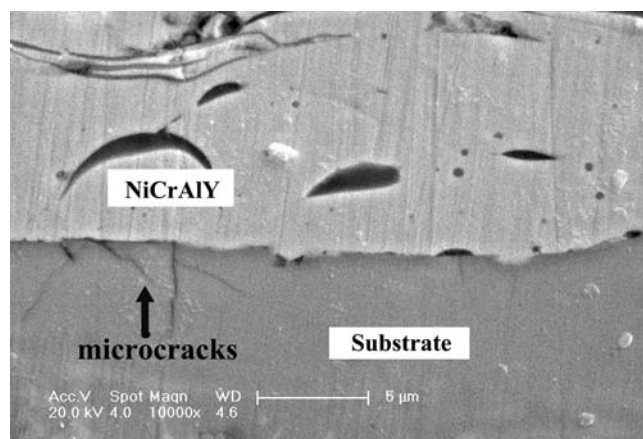


**Fig. 4** SEM cross-sectional microstructure of the polished as-sprayed coating at the bond coat/substrate interface

### 3.2 Microhardness

The mean values of microhardness at 100 g load for a dwell time of 15 s for the substrate before and after plasma spraying are  $340 \pm 14$  HV and  $405 \pm 32$  HV, respectively. It is evident that the microhardness of the substrate increases after plasma spraying. The microhardness difference for the substrate before and after plasma spraying reaches approximately 16%. As discussed in the previous section, the residual stresses which formed microcracks exist in the substrate; accordingly the increased microhardness value of the substrate after plasma spraying shows another evidence for the existence of residual stresses induced by the plasma spraying process.

Figure 5 presents the Vickers microhardness distribution after plasma spraying. The measurement points are evenly distributed along the thickness of the substrate. It can be seen that the microhardness values near the bond

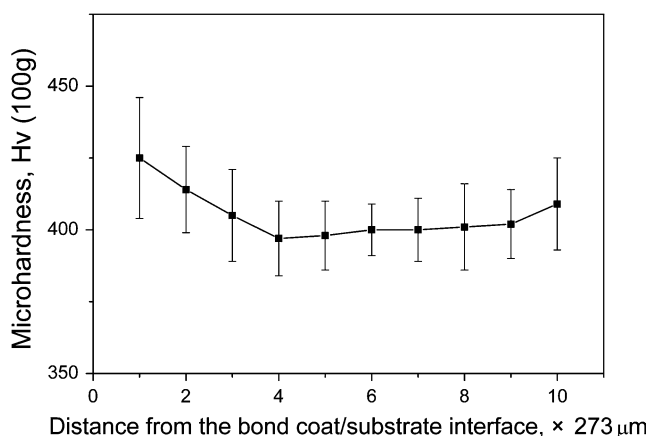


**Fig. 5** The Vickers microhardness distribution along the thickness of the substrate after plasma spraying; left is the direction to the bond coat/substrate interface. Error bars represent the standard deviations for all measurements

coat/substrate interface are obviously higher than that of the substrate inside. As we know that thermal stresses induced by thermal gradient and thermal expansion coefficients mismatch influence the substrate's mechanical properties, the area near the bond coat/substrate interface is affected by plasma spraying process directly, and the induced thermal stresses are concentrated in the area. Thus, the microhardness values in that area increased significantly. The microhardness values of the internal substrate were also influenced to get increased, but less than those near the interface. Moreover, the microhardness value near the naked surface is also slightly higher than that of the internal substrate after spraying. It may be explained that residual stresses induced by rapid cooling rate in the surface were responsible for this phenomenon.

#### 4. Conclusions

The microstructure of the titanium alloy inside the substrate keeps unchanged after plasma spraying. Neither interaction nor atomic diffusion happens at the bond

coat /substrate interface during plasma spraying. However there exists a thin layer of plastic deformation zone in the substrate beneath the bond coat/substrate interface after plasma spraying and the thickness of the plastic deformation zone is non-uniform.

The thermal stresses are induced inside the titanium alloy during plasma spraying because of the temperature gradient and the mismatch of the thermal expansion coefficients, which are partially released by cracking, and some remained in the substrate. This leads to the microcracks formed beneath the bond coat/substrate interface and the increase of microhardness value in the substrate after plasma spraying.

#### Acknowledgments

This research is sponsored by the Scientific Research Fund of Youth Teacher in Shanghai Jiaotong University. The authors are grateful to Mr. Y. Lai, the instrumental analysis center, Shanghai Jiao Tong University, for the help with SEM and helpful discussion.

#### References

1. D.W. Mckee and K.L. Luthra, Plasma Sprayed Coatings for Titanium Alloy Oxidation Protection, *Surf. Coat. Technol.*, 1993, **56**, p 109-117
2. H. Liu, S. Hao, X. Wang, and Z. Feng, Interaction of a Near  $\alpha$  Type Titanium Alloy with NiCrAlY Protective Coating at High Temperatures, *Scripta Materialia*, 1998, **39**, p 1443-1450
3. C. Tao, Q. Liu, C. Chao, and W. Zhang, Failure and Prevention of Aeronautical Titanium Alloy. National Defense Industry Press, Beijing, 2002, p 207-209, in Chinese
4. Y. Xiong, S. Zhu, and F. Wang, The Oxidation Behavior of TiAlNb Intermetallic with Coatings at 800 °C, *Surf. Coat. Technol.*, 2005, **190**, p 195-199
5. N.P. Pature, M. Gell, and E.H. Jordan, Thermal Barrier Coatings for Gas-Turbine Engine Application, *Science*, 2002, **296**, p 280-284
6. R.A. Miller, Thermal Barrier Coatings for Aircraft Engines: History and Directions, *J. Therm. Spray Technol.*, 1997, **6**, p 35-42
7. G.W. Goward, Progress in Coatings for Gas Turbine Airfoils, *Surf. Coat. Technol.*, 1998, **108-109**, p 73-79
8. Editing committee, Practical Handbook for Engineering Materials. China Machine Press, Beijing, 1989, p 652-669, in Chinese